

## A Density Functional Study of Trigold Oxonium Complexes and of Their Dimerization

Sai-Cheong Chung,<sup>†</sup> Sven Krüger,<sup>†</sup> Hubert Schmidbaur,<sup>‡</sup> and Notker Rösch<sup>\*,†</sup>

Lehrstuhl für Theoretische Chemie, Technische Universität München, 85747 Garching, Germany, and Anorganisch-chemisches Institut, Technische Universität München, 85747 Garching, Germany

Received April 17, 1996<sup>⊗</sup>

The dimerization of trigold oxonium cations has been studied theoretically by means of the all-electron scalar relativistic linear combination of Gaussian-type orbitals density functional (LCGTO-DF) approach. A partial geometry optimization of the model compounds  $[\text{OAu}_3]^+$  and  $[\text{O}(\text{AuPH}_3)_3]^+$  was carried out for these monomers as well as for their dimers, considering various aggregation modes. Additionally, the influence of the steric repulsion of larger phosphine substituents on the structure of the dimer has been examined using a force field method. Reflecting the competition between the Au–Au attraction and the interligand steric repulsion, in agreement with the experimental trends, the dimerization in a locally tetrahedral coordination is favored for the nonligated trigold oxonium cations, whereas a locally rectangular coordination is obtained for the phosphine-ligated complexes.

## 1. Introduction

Although gold is a noble metal, a rich variety of homo- and heteronuclear gold cluster compounds is known by now.<sup>1,2</sup> This is especially remarkable since only a few cluster compounds of the less noble coinage metals silver and copper have so far been synthesized.<sup>1</sup> The interesting cluster chemistry of gold has been traced in part to an attraction between formally closed shell Au(I) atoms. The term “aurophilic interaction” has been suggested for this attractive interaction,<sup>2</sup> which is also the driving force for the oligomerization of many gold(I) compounds resulting in intermolecular Au–Au contacts which are comparable to intramolecular Au–Au bond distances. Examples of species which show different forms of structural aggregation are trigold oxonium compounds.<sup>3–7</sup> This class of compounds is also of interest as a source of useful aurating agents, and it represents the basis for the synthesis of a variety of other cluster compounds.<sup>8</sup>

All trigold oxonium cations contain  $[\text{OAu}_3]^+$  moieties which form a trigonal pyramid with a  $\text{Au}_3$  base. Different phosphine ligands L have been used to synthesize species of the type  $[\text{O}(\text{AuL})_3]^+$ . If bulky ligands like tri-*o*-tolylphosphine,  $\text{P}(\text{o-tol})_3$ ,<sup>4</sup> or triisopropylphosphine,  $\text{P}^i\text{Pr}_3$ ,<sup>6</sup> are introduced, the oxonium salts crystallize with the cations as monomers. Dimerization is observed for smaller ligands. The geometry of the dimers depends on the nature of the ligands which are attached to the gold atoms. For triphenylphosphine,  $\text{PPh}_3$ , or methyl-diphenylphosphine,  $\text{PMePh}_2$ , the complexes are bound via parallel edges of the  $\text{Au}_3$  triangles, leading to an approximately rectangular  $\text{Au}_4$  subunit (“rectangular” dimer, Figure 1a).<sup>3,4</sup> Recently, with trimethylphosphine ligands,  $\text{PMe}_3$ , dimerization

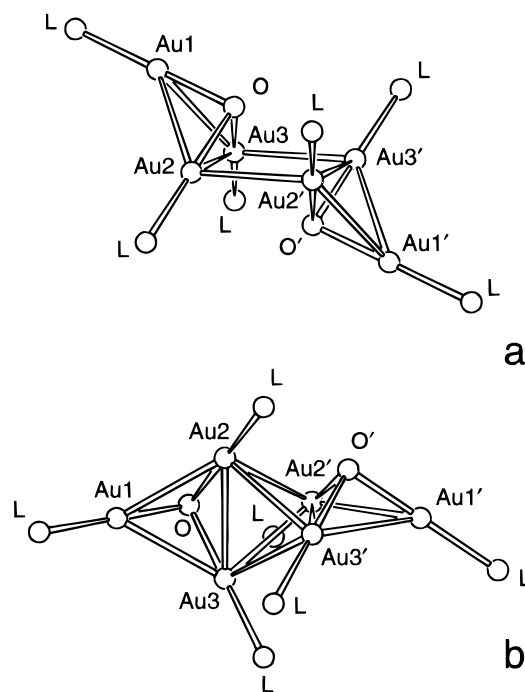


**Figure 1.** Sketches of two structures of trigold oxonium dimers: (a) rectangular; (b) tetrahedral. Phosphine ligands are indicated by L.

via crossed edges has been found, resulting in an approximately tetrahedral contact of the monomers (“tetrahedral” dimer, Figure 1b).<sup>5</sup>

The aim of the present work is to study the dimerization of trigold oxonium cations theoretically by examining the model compounds  $[\text{OAu}_3]^+$  and  $[\text{O}(\text{AuPH}_3)_3]^+$ . A partial geometry optimization of monomers and dimers, the latter both in rectangular and in tetrahedral structures, was carried out by means of an all-electron scalar relativistic density functional approach. To further elucidate the influence of intermonomer ligand repulsion on the dimerization, force field calculations have also been performed in order to estimate the steric repulsion of ligands for different dimer structures and different phosphine substituents. While the corresponding sulfonium monomers  $[\text{SAu}_3]^+$  and  $[\text{S}(\text{AuPH}_3)_3]^+$  have recently been treated by means of a Hartree–Fock-based MP2 pseudopotential method,<sup>9</sup> the present work is to our knowledge the first attempt to model the dimerization of trigold chalcogenium cations.

\* Author to whom correspondence should be addressed.

<sup>†</sup> Lehrstuhl für Theoretische Chemie, TU München.

<sup>‡</sup> Anorganisch-chemisches Institut, TU München.

<sup>⊗</sup> Abstract published in *Advance ACS Abstracts*, August 1, 1996.

- (1) Hall, K. P.; Mingos, D. M. P. *Prog. Inorg. Chem.* **1984**, *32*, 237.
- (2) Schmidbaur, H. *Gold Bull.* **1990**, *23*, 11.
- (3) Nesmeyanov, A. N.; Perevalova, E. G.; Struchkov, Y. T.; Antipin, M. Y.; Grandberg, K. I.; Dyadchenko, V. P. *J. Organomet. Chem.* **1980**, *201*, 343.
- (4) Yang, Y.; Ramamoorthy, V.; Sharp, P. R. *Inorg. Chem.* **1993**, *32*, 1946.
- (5) Angermaier, K.; Schmidbaur, H. *Inorg. Chem.* **1994**, *10*, 2069.
- (6) Angermaier, K.; Schmidbaur, H. *Acta Crystallogr.* **1995**, *C51*, 1793.
- (7) Schmidbaur, H.; Kolb, A.; Zeller, E.; Schier, A.; Beruda, H. *Z. Anorg. Allg. Chem.* **1993**, *619*, 1575.
- (8) Schmidbaur, H. *Chem. Soc. Rev.* **1995**, *24*, 391.

The paper is organized as follows: first, some details of the utilized methods will be given, and then results for the trigold oxonium monomer will be presented followed by a discussion of the results on the dimers.

## 2. Computational Details

The electronic structure calculations have been carried out with the help of the first-principles all-electron linear combination of Gaussian-type orbitals density functional (LCGTO-DF) method.<sup>10</sup> Scalar relativistic effects including the mass-velocity correction and the Darwin term have been treated in a self-consistent fashion.<sup>11–13</sup> For the exchange-correlation potential the local density approximation (LDA) was chosen in the parametrization suggested by Vosko, Wilk, and Nusair.<sup>14</sup> For gold compounds this approximation of the exchange-correlation energy functional was shown to yield structural results comparable to those of functionals which employ corrections based on density gradients;<sup>15</sup> however, binding energies, as is often observed, may be calculated too large in the LDA approach.

For Au, P, and H the same orbital basis sets have been used as in previous studies on MeAuPR<sub>3</sub><sup>16</sup> and on main-group element-centered X(AuL)<sub>n</sub> clusters (*n* = 4–6).<sup>17</sup> For oxygen we employed an orbital basis set consisting of 9 s-, 5 p-, and 1 d-type exponents.<sup>18,19</sup> All orbital basis sets were contracted in a generalized fashion using atomic LDA eigenvectors. The resulting atomic orbital basis sets and their contractions were (21s,17p,11d,7f) → [11s,10p,7d,3f] for Au, (12s,9p,1d) → [8s,6p,1d] for P, and (9s,5p,1d) → [5s,4p,1d] for C and O, as well as (6s,1p) → [4s,1p] for H. The fitting basis sets employed in the LCGTO-DF approach to represent the electronic charge density and the exchange-correlation potential were constructed in a standard fashion by scaling orbital exponents.<sup>10,16</sup> To reduce the computational effort, only s- and p-type functions were included in the fitting basis sets.

The steric repulsion between the ligand shells of trigold oxonium dimers, in particular the effect of different phosphine substituents, was estimated with the help of a force field model. We employed the universal force field approach (UFF)<sup>20,21</sup> which uses mainly atom-based parameters.<sup>20</sup> In the UFF approach, these are used to determine the interatomic forces instead of a direct parametrization of force terms common in many other force field methods. The present UFF method also comprises the so-called VALBOND approach<sup>22</sup> and a charge equilibration scheme.<sup>23</sup> The former methodology accounts in a flexible way for effects of atomic hybridization while the latter provides a description of the Coulomb interaction in a molecule due to partially charged atoms.

## 3. The Trigold Oxonium Monomer

For the electronic structure investigations, the complex [O(AuPH<sub>3</sub>)<sub>3</sub>]<sup>+</sup> has been taken to model experimentally available trigold oxonium cations which contain larger phosphine substituents.<sup>3–5</sup> As shown previously,<sup>16</sup> unsubstituted phosphine, PH<sub>3</sub>, may profitably be used as a model ligand to reduce the computational effort when structural aspects are concerned.

**Table 1.** Comparison of Calculated and Experimental Bond Distances (in Å) of Trigold Oxonium Monomer Moieties

system	<i>d</i> (Au–Au)	<i>d</i> (Au–O)	<i>d</i> (Au–P)
	Calculated		
Au <sub>3</sub> <sup>+</sup>	2.56		
[O(Au <sub>3</sub> ) <sup>+</sup>	2.78	2.02	
[O(AuPH <sub>3</sub> ) <sub>3</sub> ] <sup>+</sup>	2.88	2.02	2.17
	Experimental <sup>a</sup>		
monomers, rectangular dimers <sup>b</sup>	3.05–3.09	1.97–2.05	2.22–2.26
monomer with L = P <sup>i</sup> Pr <sub>3</sub> <sup>c</sup>	3.20	2.03	2.23
tetrahedral dimer <sup>d</sup>	3.31	2.02	2.22

<sup>a</sup> Averaged values. <sup>b</sup> References 3 and 4. <sup>c</sup> Reference 6. <sup>d</sup> Reference 5.

For the Au<sub>3</sub> moiety an equilateral triangular shape was assumed, in close agreement with experimental findings. [O{AuP(*o*-tol)<sub>3</sub>}<sub>3</sub>]<sup>+</sup> exhibits deviations from the 60° angle of an equilateral triangle by only 0.3°;<sup>4</sup> in other trigold oxonium cations deviations up to 2–4° have been noted.<sup>3–5</sup> Thus the present structural idealization does not impose a severe restriction. A partial geometry optimization was carried out for [O(AuPH<sub>3</sub>)<sub>3</sub>]<sup>+</sup>, imposing C<sub>3v</sub> symmetry. The distance *d*(Au–Au), the height of the O atom above the Au triangle, and the distance *d*(Au–P) were optimized. For the phosphine ligands a fixed geometry was used, with *d*(P–H) = 1.415 Å and ∠(H–P–H) = 93.3°.<sup>24</sup> The angle P–Au–O was kept fixed at 180°, corresponding to the preferred linear geometry of Au(I) complexes. Experimentally, the mean value of this angle is 178.4° in [O{AuP(*o*-tol)<sub>3</sub>}<sub>3</sub>]<sup>+</sup>;<sup>4</sup> in dimers it is found to be up to 5° smaller.<sup>3–5</sup> Since no analytic energy gradients were available in the scalar relativistic variant of the LCGTO-DF method, a cyclic optimization strategy had to be employed. Thereby, the minimum along each investigated degree of freedom was determined from a series of single point calculations until all structural parameters were stable to less than 0.002 Å.

The optimized bond lengths of [O(AuPH<sub>3</sub>)<sub>3</sub>]<sup>+</sup> are given in Table 1 together with those obtained for the unligated compound [O(Au<sub>3</sub>)<sup>+</sup> and the gold trimer Au<sub>3</sub><sup>+</sup>. The Au–Au bond in Au<sub>3</sub><sup>+</sup>, *d*(Au–Au) = 2.56 Å, is nearly 0.1 Å longer than the calculated and experimental results for neutral diatomic Au<sub>2</sub>, *d*(Au–Au) = 2.47 Å.<sup>13,25</sup> The addition of O leads to a considerable increase of the Au–Au distance, *d*(Au–Au) = 2.78 Å, establishing a nearly optimal angle Au–O–Au of 87.0° for employing the p orbitals of oxygen in the bonding. When the phosphine ligands are taken into account, a further elongation of the Au–Au bond is observed, *d*(Au–Au) = 2.88 Å, while the Au–O distance remains unchanged, *d*(Au–O) = 2.02 Å. A comparison of the optimized Au–P distance, *d*(Au–P) = 2.17 Å, with the one in MeAuPH<sub>3</sub>, *d*(Au–P) = 2.29 Å,<sup>16</sup> reveals that the stronger acceptor character of [O(Au<sub>3</sub>)<sup>+</sup> as compared to AuMe leads to a considerably shorter bond. The computed binding energy per phosphine ligand is –3.61 eV in [O(AuPH<sub>3</sub>)<sub>3</sub>]<sup>+</sup>, which is not much smaller than the value for an isolated [AuPH<sub>3</sub>]<sup>+</sup> unit, –4.15 eV.<sup>16</sup> This confirms that the gold atoms in [O(AuPH<sub>3</sub>)<sub>3</sub>]<sup>+</sup> have to be considered in a +I oxidation state. For neutral AuPH<sub>3</sub>, the phosphine bond is significantly weaker, –1.28 eV.<sup>16</sup> The O binding energy amounts to –3.08 eV in the cluster [O(Au<sub>3</sub>)<sup>+</sup>. This bond is strengthened considerably by the addition of ligands due to the donor character of the phosphine groups. For the ligand trigold oxonium cluster the calculated oxygen binding energy is –6.22 eV. The Au–Au interaction

- (9) Pyykkö, P.; Angermaier, K.; Assmann, B.; Schmidbaur, H. *J. Chem. Soc., Chem. Commun.* **1995**, 1889.
- (10) Dunlap, B. I.; Rösch, N. *Adv. Quantum Chem.* **1990**, 21, 317.
- (11) Knappe, P.; Rösch, N. *J. Chem. Phys.* **1990**, 92, 1153.
- (12) Rösch, N.; Häberlen, O. D. *J. Chem. Phys.* **1992**, 96, 6322.
- (13) Häberlen, O. D.; Rösch, N. *Chem. Phys. Lett.* **1992**, 199, 491.
- (14) Vosko, S. H.; Wilk, L.; Nusair, M. *Can. J. Phys.* **1980**, 58, 1200.
- (15) Mayer, M.; Rösch, N. To be published.
- (16) Häberlen, O. D.; Rösch, N. *J. Phys. Chem.* **1993**, 97, 4970.
- (17) Häberlen, O. D.; Schmidbaur, H.; Rösch, N. *J. Am. Chem. Soc.* **1994**, 116, 8241.
- (18) Van Duijneveldt, F. B. *IBM Res. Rep. RJ* **1971**, 945.
- (19) Huzinaga, S. Ed. *Gaussian Basis Sets for Molecular Calculations*; Elsevier: New York, 1984.
- (20) Rappe, A. K.; Casewit, C. J.; Colwell, K. S.; Goddard, W. A., III; Skiff, W. M. *J. Am. Chem. Soc.* **1992**, 114, 10024.
- (21) Rappe, A. K.; Colwell, K. S.; Casewit, C. J. *Inorg. Chem.* **1993**, 32, 3438.
- (22) Root, D.; Landis, C. R.; Cleveland, T. *J. Am. Chem. Soc.* **1993**, 115, 4201.
- (23) Rappe, A. K.; Goddard, W. A., III *J. Phys. Chem.* **1991**, 95, 3358.

- (24) Weast, R. C., Ed., *CRC Handbook of Chemistry and Physics*, 64th ed., CRC Press: Boca Raton, FL, 1983.
- (25) Huber, K. P.; Herzberg, G. *Molecular Spectra and Molecular Structure. Constants of Diatomic Molecules*; Van Nostrand: New York, 1979; Vol. 4.

cannot be studied directly in the trigold oxonium cations because it is difficult to partition these clusters in a meaningful fashion. For dimers of two  $\text{XAuPH}_3$  moieties, an attractive Au–Au interaction of up to 0.25 eV has been calculated,<sup>26</sup> depending on the ligand X; estimates from NMR experiments yield up to 0.4 eV.<sup>27–30</sup>

Compared to experiment the Au–P and Au–O distances agree reasonably well, while the Au–Au distance is calculated somewhat too short. This leads to an underestimation of the angle Au–O–Au, the mean value of which varies between 96 and 104° in experiment.<sup>3,4,6</sup> but is calculated to 90.6°. The only tetrahedrally dimerizing complex  $[\text{O}(\text{AuPMe}_3)_3]^+$  exhibits the extreme value of 110° for the angle Au–O–Au,<sup>5</sup> as a consequence of the relatively large Au–Au distances (see Table 1). However, it has to be taken into account that all trigold oxonium compounds with small ligands tend to dimerize and that only species with bulky ligands are obtained as monomers. Thus, the effects of dimerization and packing as well as of the crystal field render a straightforward and detailed comparison of experimental and computed structural parameters difficult.

Recently, the sulfonium analogs of the model compounds examined in this work have been treated at the MP2 level of ab initio methodology employing appropriate pseudopotentials to account for relativistic effects.<sup>9</sup> Only the Au–S–Au angle has been optimized in that study. It was found to be about 83° for both “naked” and phosphine-ligated  $[\text{SAu}_3]^+$  cations. Experimental results for  $\text{PPh}_3$  and  $\text{P}^i\text{Pr}_3$  ligated trigold sulfonium monomers<sup>9</sup> confirm a smaller Au–S–Au angle in comparison to the oxonium compounds. This finding is mainly due to the larger size of the S atom and the correspondingly longer S–Au bond distance (2.32 Å) compared to O–Au. As in our study, the Au–Au bond length was calculated shorter than that found in experimentally characterized compounds, which contain larger ligands.<sup>9</sup>

While the Au centers in trigold chalcogenium compounds are considered to be formally closed shell 5d<sup>10</sup> Au(I) ions, the Mulliken population analysis yields a somewhat different picture. For  $[\text{O}(\text{AuPH}_3)_3]^+$  the Au configuration is  $6s^{0.98}6p^{0.31}-5d^{9.39}5f^{0.05}$ . The 6s occupation corresponds to the atomic value, and even the 6p orbitals are populated due to hybridization. These results show that the 5d shell is not completely closed and that it thus may contribute to the metal–metal bonding, as has previously been noted for other gold–phosphine compounds.<sup>16,31–33</sup> Finally, we mention that the Mulliken analysis is in qualitative agreement with the Hartree–Fock results for the corresponding sulfonium compound where a Au configuration of  $6s^{0.88}6p^{0.63}5d^{9.63}5f^{0.07}$  was determined.<sup>9</sup>

#### 4. The Trigold Oxonium Dimer

**4.1. Optimization of Dimer Geometries.** A full geometry determination of trigold oxonium dimers with a first-principles all-electron approach is extremely demanding. Thus, we have considered the monomeric subunits in their optimized geometry

**Table 2.** Comparison of Calculated and Experimental Intermonomer Au–Au' Distances (in Å) for Trigold Oxonium Dimers of Rectangular and Tetrahedral Structures (See Figure 1)

system	$d(\text{Au}-\text{Au}')$	
	rect	tetrah
$[\text{OAu}_3]_2^{2+}$	2.80	2.89
$[\text{O}(\text{AuPH}_3)_3\text{O}]_2^{2+}$	3.0 <sup>a</sup>	3.00
exptl	3.06–3.16 <sup>b</sup>	3.27 <sup>c</sup>

<sup>a</sup> Quoted to one digit only because of the very shallow potential curve which does not allow a more accurate determination. <sup>b</sup> References 3 and 4. <sup>c</sup> Reference 5, average value.

**Table 3.** Binding Energies,  $\text{BE} = E(\text{dimer}) - 2E(\text{monomer})$  (in eV), of Trigold Oxonium Dimers for the Tetrahedral and the Rectangular Structures Calculated without and with Point Charge (PC) Models of the Crystal Environment

system	BE		$\Delta\text{BE}^a$ rect – tetrah
	rect	tetrah	
$[\text{OAu}_3]_2^{2+}$	1.57	1.30	0.27
$[\text{OAu}_3]_2^{2+} + 2\text{PC}$	–0.87	–1.04	0.17
$[\text{OAu}_3]_2^{2+} + 8\text{PC}$	–1.62	–1.78	0.16
$[\text{O}(\text{AuPH}_3)_3]_2^{2+}$	2.23	5.45	–3.22
$[\text{O}(\text{AuPH}_3)_3]_2^{2+} + 2\text{PC}$	–1.39	1.62	–3.01
$[\text{O}(\text{AuPH}_3)_3]_2^{2+} + 8\text{PC}$	–1.91	0.85	–2.76

<sup>a</sup> Negative values of BE indicate a preference for the rectangular geometry.

and restricted the present study to an optimization of the interdimer distance. Even this is a challenging task since four to six symmetry inequivalent gold atoms have to be treated, depending on the structure and the symmetry of the dimer.

As discussed in the introduction, two dimer structures are of interest, the “rectangular” and the “tetrahedral” one (Figure 1). When modeling the first case, the dimer geometry has been slightly idealized to preserve  $C_{2h}$  symmetry (Figure 1a) by adopting a perfect rectangular shape of the contact unit and by appropriately orientating the H atoms of the phosphine ligands. The  $C_2$  axis passes perpendicularly through the two Au–Au' bonds which connect the monomeric subunits. For the tetrahedral dimer (Figure 1b)  $C_2$  symmetry has been used, as found experimentally for the trigold oxonium cation with  $\text{PMe}_3$  ligands.<sup>5</sup> Additionally, the edges of the  $\text{Au}_3$  triangles connecting the monomer moieties were chosen to be perpendicular to each other; the corresponding experimental angle amounts to 90.3°.<sup>5</sup> For this geometry, too, the  $C_2$  axis passes perpendicularly through two of the intermonomer Au–Au' contacts (cf. Figure 2b). The  $\text{Au}_3$  triangles of the monomers were oriented according to experimental data; see ref 3 for the rectangular dimer with  $\text{L} = \text{PPh}_3$  and ref 5 for the tetrahedral dimer.

The optimization results for the intermonomer distance are shown in Table 2. In both structures the Au–Au' distance is elongated by 0.1–0.2 Å when  $\text{PH}_3$  ligands are added to the  $[\text{OAu}_3]_2^{2+}$  core of the complex. In case of the rectangular dimer, the calculated bond length is somewhat smaller than the values observed experimentally for complexes with considerably larger ligands.<sup>3,4</sup> For the tetrahedrally coordinated dimer, a large underestimation of the measured Au–Au' distance by about 0.3 Å has to be noted.

The calculated binding energies,  $\text{BE} = E\{[\text{O}(\text{AuL})_3]_2^{2+}\} - 2E\{[\text{O}(\text{AuL})_3]^+\}$ , of the dimers in the rectangular and tetrahedral structure are compared in Table 3; negative values of BE correspond to an exothermic reaction  $2[\text{O}(\text{AuL})_3]^+ \rightarrow [\text{O}(\text{AuL})_3]_2^{2+}$ . For both the “naked” and the ligated clusters, a positive BE value (no binding) was calculated, although a minimum was located on all potential energy curves. Obviously, this overall repulsive behavior is due to the Coulomb

- (26) Pyykkö, P.; Li, J.; Runeberg, N. *Chem. Phys. Lett.* **1994**, *218*, 133.  
 (27) Schmidbaur, H.; Graf, W.; Müller, G. *Angew. Chem., Int. Ed. Engl.* **1988**, *27*, 417.  
 (28) Dziwok, K.; Lachmann, J.; Wilkinson, D. L.; Müller, G.; Schmidbaur, H. *Chem. Ber.* **1990**, *123*, 423.  
 (29) Schmidbaur, H.; Dziwok, K.; Grohmann, A.; Müller, G. *Chem. Ber.* **1989**, *122*, 893.  
 (30) Harwell, D. E.; Mortimer, M. D.; Knobler, C. B.; Anet, F. A.; Hawthorne, M. F. *J. Am. Chem. Soc.* **1996**, *118*, 2679.  
 (31) DeKock, R. L.; Baerends, E. J.; Boerrigter, P. M.; Hengelmolen, R. *J. Am. Chem. Soc.* **1984**, *106*, 3387.  
 (32) Rösch, N.; Görling, A.; Ellis, D.; Schmidbaur, H. *Angew. Chem., Int. Ed. Engl.* **1989**, *28*, 1357.  
 (33) Görling, A.; Rösch, N.; Ellis, D. E.; Schmidbaur, H. *Inorg. Chem.* **1981**, *30*, 3986.

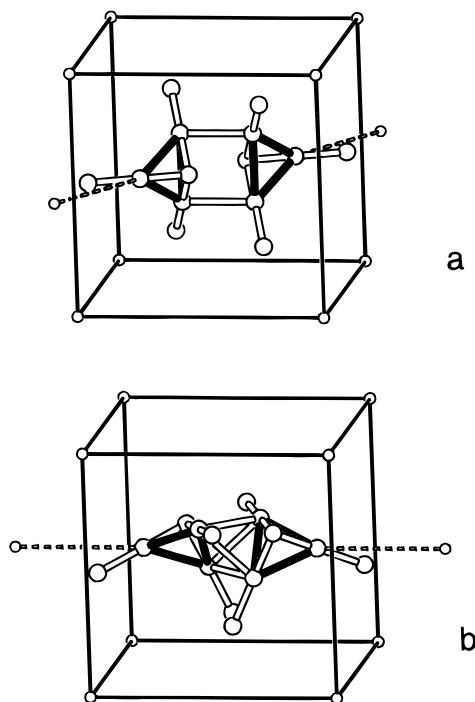


**Figure 2.** Point charge (PC) models for the Madelung field set up by the counterions around the trigold oxonium dimer dication: (a) rectangular dimer; (b) tetrahedral dimer. The location of the point charges is indicated by dashed lines (2-PC model) and by solid lines (8-PC model). For each structure both PC models are superimposed in the sketches for ease of comparison.

interaction between the charged monomer species. The differences of the binding energies show that the dimer of “naked”  $[\text{O}(\text{Au}_3)]^+$  moieties is more stable in the tetrahedral structure, but for the ligated monomers the rectangular dimerization is energetically favored. This clear preference of the rectangular structure for the ligated clusters will have to be reconsidered in the light of the results for the steric interaction of ligands; see below. Nevertheless, these results reflect the experimental tendency toward a tetrahedral dimerization for smaller ligands, although the crystal environment has not been taken into account in these model calculations.

The interaction between the monomers is too small to noticeably change their electronic structure. Thus, no significant changes in the Mulliken populations ( $<0.1$ ) and in the effective configuration of the Au atoms are induced by the dimerization. Only the 6p population is enhanced by up to 0.1 for those gold atoms, which are directly involved in the intermonomer bonding.

**4.2. Stabilization of Dimers in the Crystal Field.** To simulate in an approximate fashion the stabilization of the dications in the crystal environment, two different point charge (PC) models have been constructed, in order to represent the Madelung field set up by the counterions. Both models are sketched in Figure 2. The first model features two point charges (charge  $q = +1.0$  au), which were placed on the line connecting the center of the  $\text{Au}_3$  triangle with the midpoint of the  $\text{Au}_2$ – $\text{Au}_3$  edge involved in the dimer bonding (see Figure 1). In both dimer structures, the distance of point charges from the center of the  $\text{Au}_3$  triangle was fixed at 8.23 Å according to the experimental findings for  $[\text{O}(\text{AuPMe}_3)_3]_2^{2+}[\text{BF}_4^+]_2$ .<sup>5</sup> An alternative model for the Madelung field was constructed by uniformly distributing the necessary counter charge over the corners of a cube ( $q = +0.25$  au). The length of the cube edges (11.64 Å) was chosen so that half of the face diagonal amounts to 8.23 Å. This second model leads to a weaker Madelung field since the Au–PC distances are all slightly larger than the

corresponding distances in experiment and in the first PC model. The dimers inside the cube were oriented so that the  $C_2$  axis of the dimer complex passes through the midpoints of two opposite faces of the cube; furthermore, for both dimer structures a line perpendicular to the  $C_2$  axis and intersecting the bonds  $\text{Au}_2$ – $\text{Au}_3$  passes through the center of another pair of opposite cube faces (see Figures 1 and 2). The binding energies were determined for the dimers in the optimized (monomer) geometries which have been discussed above. To obtain the total energy of the monomer in the first PC model, the monomer was neutralized by including one of the point charges; in the second PC model, the monomer was surrounded by a cube of the same size, but with the value of point charges appropriately reduced ( $q = +0.125$  au).

Inspection of Table 3 shows that the calculated values of the dimer binding energy depend considerably on the point charge model chosen. The values change up to 100%. For all dimers, except for the ligated tetrahedral one, negative binding energies are obtained. Although the absolute binding energies differ substantially, close agreement is found for the binding energy differences between the rectangular and tetrahedral dimer structures. These values are also in good agreement with the slightly higher binding energy differences calculated without any counter charges. Nevertheless, the conclusions concerning the preferred dimerization structure as stated above are corroborated by both point charge models: for the bare trigold oxonium complex a tetrahedral dimerization is more stable, while after addition of phosphine ligands the rectangular structure is considerably favored. The calculated preferences parallel the experimental trend. A tetrahedral dimer structure has been observed only for the complex with the least bulky ligand synthesized so far,  $\text{PMe}_3$ .<sup>5</sup> There may be several reasons why the calculations favor a rectangular dimerization already for  $\text{PH}_3$ , whereas the experimental findings suggest a tetrahedral structure for such small ligands. As will be shown in the following, one of them is an overestimation of the steric repulsion between the ligands due to the underestimated Au–Au and Au–Au' distances in the optimized structures.

**4.3. Steric Interaction of the Ligand Shells.** To further elucidate the influence of steric repulsion on the dimerization of trigold oxonium cations, we have performed calculations on the neutral ligand shells alone (no point charges were included), arranged according to the optimized dimer structures. The ligand repulsion has also been determined for experimental geometries to probe the effect of our geometric idealizations. The ligands of the monomeric subunits are well separated, while after dimerization, the ligands belonging to two different monomers may come quite close (see Figure 1). Thus, the main contribution to the ligand repulsion should arise from intermonomer contacts. While one may only treat models with  $\text{PH}_3$  ligands at a reasonable calculational effort by means of the LCGTO-DF method, a force field approach allows also the examination of the more bulky ligands  $\text{PMe}_3$  and  $\text{PPh}_3$ . The experimental structures were chosen according to  $[\text{O}(\text{AuPMe}_3)_3]_2^{2+}$  for the tetrahedral dimer<sup>5</sup> and according to  $[\text{O}(\text{AuPPh}_3)_3]_2^{2+}$  for the rectangular dimer.<sup>3</sup> In these modeling calculations the H atoms of the phenyl rings were located by assuming a C–H bond length of 1 Å and a C–C–H angle of 120°.

Besides the negligible differences in the Au–O and Au–P distances ( $<0.1$  Å), the experimental geometries exhibit longer Au–Au distances as the most prominent differences to the calculated optimized structures. For the rectangular dimer the intramonomer Au–Au bond length is increased by 0.21 Å, leading to an Au–O–Au angle of 103° compared to 90.6° in

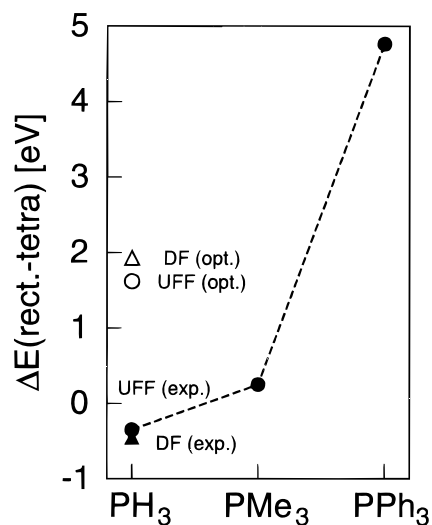


**Figure 3.** Total energy difference  $\Delta E$  of the dimer ligand shell in the rectangular and the tetrahedral structure for various types of phosphine ligands: triangles, LCGTO-DF method; circles, UFF method; open symbols, optimized geometries; filled symbols, experimental geometries. Note: positive values of  $\Delta E$  indicate a preference for the rectangular geometry.

the optimized monomer geometry. The intermonomer distance increases by 0.16 Å. For the tetrahedral dimer the differences are more pronounced: The intramonomer Au–Au bond is 0.42 Å longer, leading to an opening of the Au–O–Au angle to 110°; the intermonomer Au–Au' distance is elongated by 0.27 Å (compare Tables 1 and 2). Both effects, the increase in the Au–O–Au angle and the elongation of the intermonomer distance, result in enhanced ligand separation, which should decrease the steric repulsion. As an indication for the steric crowding in the idealized dimer structures which are based on the optimized monomer geometry, we mention that the shortest H–H contact amounts to 1.7 Å for the tetrahedral geometry. It is elongated to 3.6 Å in the experimentally determined structure. The slight idealization of the tetrahedral contact of the monomers should be of minor importance since in the experimental tetrahedral geometry the edges of the Au<sub>3</sub> triangles are also essentially perpendicular (90.3°).<sup>5</sup>

Density functional calculations on the isolated PH<sub>3</sub> ligands, arranged according to the four dimer geometries, show that the ligand repulsion for the tetrahedral dimer decreases by 2.1 eV when going from the optimized to the experimental geometry. For the rectangular dimer, on the other hand, the ligand arrangement of the optimized geometry is favored by 0.3 eV. Elongation of the Au–Au distances leads to a strong decrease of steric repulsion, thus rationalizing the exceptionally large Au–Au bond length measured for the tetrahedral dimers of [O(AuPMe<sub>3</sub>)<sub>3</sub>]<sup>+</sup>.<sup>5</sup> The strong deviations between experiment and our calculational results with respect to the Au–Au bond lengths can also be understood by the ligand repulsion, since a relaxation of the preoptimized monomer geometries was not included in the geometry determination of the dimers. It is worth noting that the reduction of the steric repulsion by 2.1 eV for the ligated dimer in the tetrahedral geometry leads to an interunit bonding (see Table 3), independent of the point charge model used.

After the ligand repulsion differences between experimental and optimized structures have been discussed, the differences between tetrahedral and rectangular dimers have to be considered. In Figure 3, the energy differences between ligand shells of rectangular and tetrahedral dimers are displayed for different ligand species. The LCGTO-DF calculations show that the ligand repulsion of the tetrahedral dimer with PH<sub>3</sub> ligands is

larger by 1.93 eV if the optimized geometries are used. For the experimental geometries, this difference between the two dimer geometries decreases considerably. The steric interaction in the tetrahedral dimer is even lower by 0.45 eV. Due to the small energy difference found, the preference of the tetrahedral dimer structure of trigold oxonium with small phosphine ligands, which may be inferred from the experimentally observed tetrahedral structure even for the larger ligands PMe<sub>3</sub>, can not exclusively be attributed to a difference in the electronic and steric interaction between the monomers. Crystal packing effects also have to be considered. Thus, the present density functional results do not exclude that [O(AuPH<sub>3</sub>)<sub>3</sub>]<sup>+</sup> dimerizes in the rectangular structure when placed in a suitable crystal environment. The total change in the difference of the ligand repulsion amounts to 2.4 eV when optimized and experimental geometries are compared. This accounts for most of the energy by which the rectangular geometry is favored according to the LCGTO-DF results for [O(AuPH<sub>3</sub>)<sub>3</sub>]<sub>2</sub><sup>2+</sup> (about 3 eV, see Table 3).

The rather weak influence of the steric repulsion on the structure of the trigold oxonium dimers with small phosphine ligands is further confirmed by the UFF results for the ligand repulsion, see Figure 3. In the case of simple phosphine, PH<sub>3</sub>, the force field results nicely agree with those of the more accurate LCGTO-DF calculations, for both the experimental and the optimized geometries. In both cases, the DF and the UFF results differ at most by 0.3 eV, exemplifying the quality of the UFF approach for the description of nonbonding interactions. For PMe<sub>3</sub> ligands in the experimental geometry, a slight preference for the rectangular dimer is calculated. As for the PH<sub>3</sub> ligated complexes, one may conclude that for PMe<sub>3</sub> ligands the experimentally found tetrahedral dimer should have a stability similar to that of the rectangular one. There are also indications from experiment that skeletal rearrangements meet only low energy barriers.<sup>5</sup> Thus, also for PMe<sub>3</sub> crystal packing effects have an impact on the structure in addition to the direct intermonomer interaction. If the geometry optimized for PH<sub>3</sub> is used in the case of the PMe<sub>3</sub> ligands, an unreasonably strong repulsion results in the tetrahedral structure. This clearly shows that the structural parameters determined for phosphine ligands with smaller substituents are in the present context not suitable for modeling complexes with bulkier ligands. When going from PMe<sub>3</sub> to PPh<sub>3</sub>, the steric repulsion becomes dominant. For these bulkier ligands the rectangular structure is clearly favored (see Figure 3) in agreement with experimental findings.<sup>3,4</sup>

## 5. Conclusions

The first-principles all-electron scalar relativistic LCGTO-DF method has been applied to the trigold oxonium cations [OAu<sub>3</sub>]<sup>+</sup> and [O(AuPH<sub>3</sub>)<sub>3</sub>]<sup>+</sup> and to their dimers. Additionally, force field calculations have been carried out to estimate the steric intermonomer repulsion due to the ligands PH<sub>3</sub>, PMe<sub>3</sub>, and PPh<sub>3</sub> arranged according to the different dimer geometries.

A partial optimization of the trigold oxonium monomer without and with phosphine ligands yields calculated Au–Au distances that are somewhat shorter than in experiment, but Au–O and Au–P distances are in agreement with measured bond lengths of different trigold oxonium complexes. The optimized geometries have been used to study the dimerization. For [OAu<sub>3</sub>]<sup>+</sup>, the tetrahedral dimerization was calculated to be slightly favorable, while the addition of phosphine ligands leads to the preference of a rectangular dimer structure. These results hold also if the stabilizing effect of the Madelung field set up by counterions is taken into account by means of point charge models.

To gain further insight in the mechanisms determining the dimer structures, the intermonomer repulsion of the ligand shell was calculated by arranging neutral ligands according to the different trigold oxonium dimer geometries. On the basis of LCGTO-DF results one estimates that about 80% of the binding energy difference between the rectangular and tetrahedral dimer structures with  $\text{PH}_3$  ligands are due to differences in the intermonomer repulsion of the ligand shells. In the experimental geometry of the phosphine ligand shell, the difference in steric repulsion is significantly lower and the tetrahedral geometry is even slightly favored. UFF force field calculations show that the rectangular structure exhibits a somewhat smaller steric repulsion for  $\text{PMe}_3$  ligands. For the larger  $\text{PPh}_3$  substituents, the rectangular dimer structure is calculated to clearly provide less steric crowding.

Summarizing the density functional and the molecular modeling calculations, we note that the experimental rectangular dimer structure of  $[\text{O}(\text{AuPPh}_3)_3]_2^{2+}$  is mainly determined by steric intermonomer repulsion. On the other hand, for  $[\text{O}(\text{AuPMe}_3)_3]_2^{2+}$ , which dimerizes tetrahedrally according to experiment, and for  $[\text{O}(\text{AuPH}_3)_3]_2^{2+}$ , crystal packing effects should play a decisive role because the intermonomer ligand repulsion differs only in a minor way between the rectangular and the tetrahedral structures. The calculated preference for the rectangular dimer structure for  $[\text{O}(\text{AuPH}_3)_3]_2^{2+}$  is consistent with these findings if the shortcomings of the partial geometry optimization are taken into account. To reiterate, the small

differences found for the steric repulsion between both structures do not allow a decisive prediction of the dimer geometry for  $[\text{O}(\text{AuL})_3]_2^{2+}$  for the ligands  $\text{L} = \text{PH}_3$  and  $\text{PMe}_3$  without additionally taking into account effects of the crystal lattice. It should be noted that cations  $[\text{S}(\text{AuPPh}_3)_3]^+$  can be found as monomers<sup>7</sup> or as (rectangular) dimers<sup>34</sup> in the crystal lattice depending on the nature of the counterion ( $\text{BF}_4^-$  or  $\text{PF}_6^-$ , respectively). These findings hold no surprises considering the results of the present study. Nevertheless, we were able to demonstrate a trend in the preference from the rectangular to the tetrahedral dimer structure in trigold oxonium complexes as the spacial requirements of the phosphine ligands decrease. Irrespective of the point charge model used to simulate the Madelung field of the crystalline environment, ligand-free  $[\text{OAu}_3]^+$  complexes prefer to dimerize with a locally tetrahedral  $\text{Au}-\text{Au}'$  contact.

**Acknowledgment.** We are indebted to Prof. C. R. Landis for providing his UFF molecular modeling package and to Dr. J. Hahn for performing the UFF calculations. This work has been supported by the Deutsche Forschungsgemeinschaft and by the Fonds der Chemischen Industrie. S.C.C. is grateful to the Deutscher Akademischer Austauschdienst for a graduate student scholarship.

IC960418R

(34) Jones, P. G.; Lensch, C.; Sheldrick, G. M. *Z. Naturforsch. B* **1982**, *37*, 141.